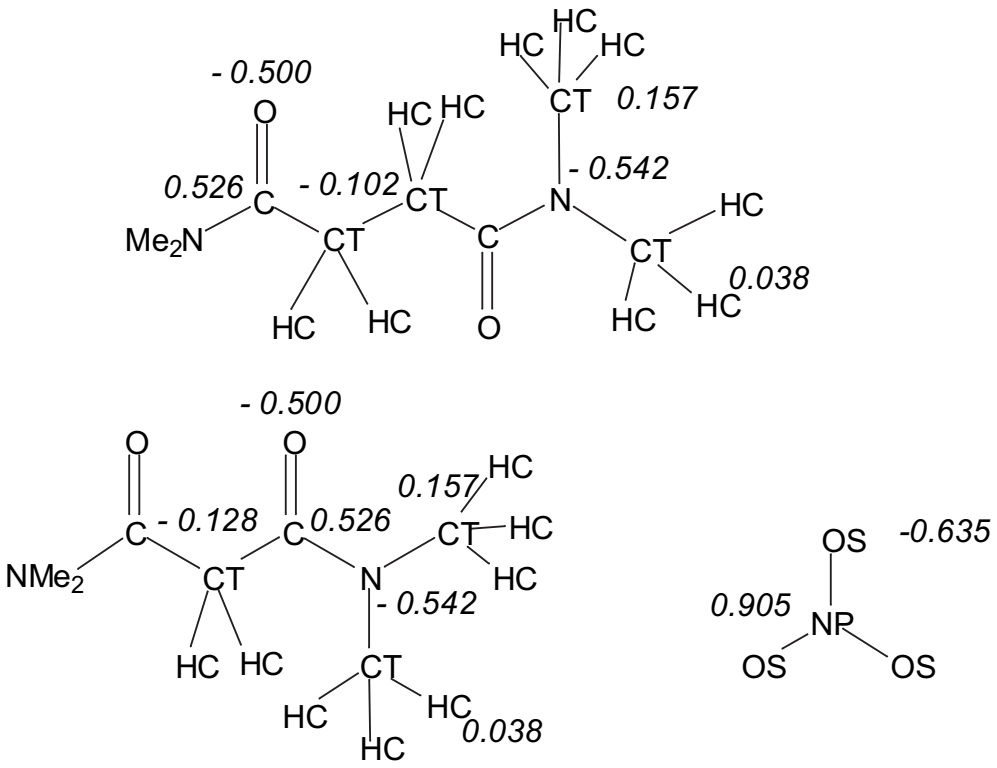

Figure S1. Atomic charges (in cursive script) and AMBER atom types used to simulate the AcA and AccA complexes and NO_3^-.

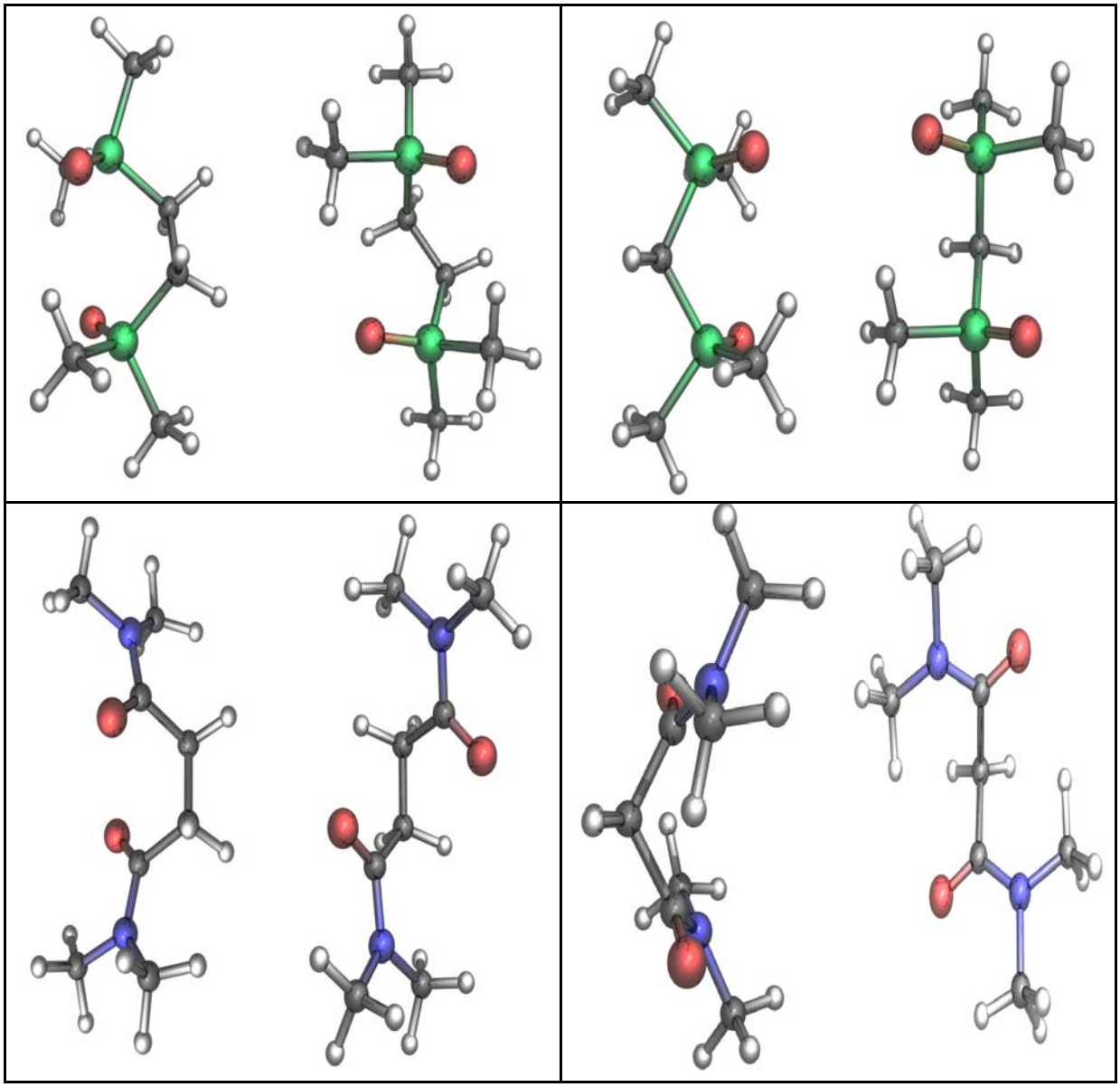

Figure S2. Optimized **L** ligands (orthogonal views). From top left to bottom right: **L** = PccP, PcP, AccA and AcA.

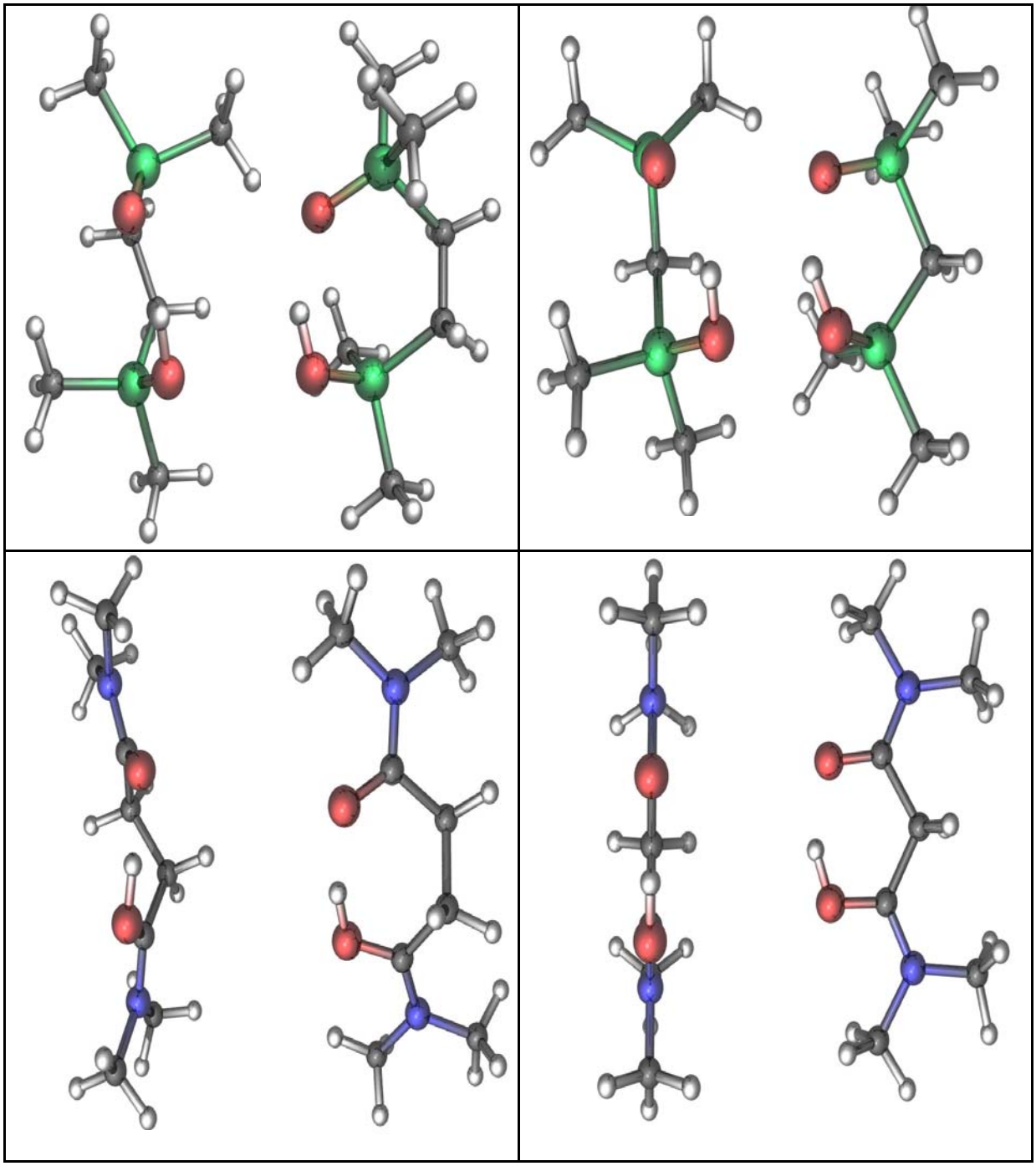

Figure S3. Optimized protonated $\mathbf{L}\cdot H^+$ ligands (orthogonal views). From top left to bottom right: **L** = PccP, PcP, AccA and AcA.

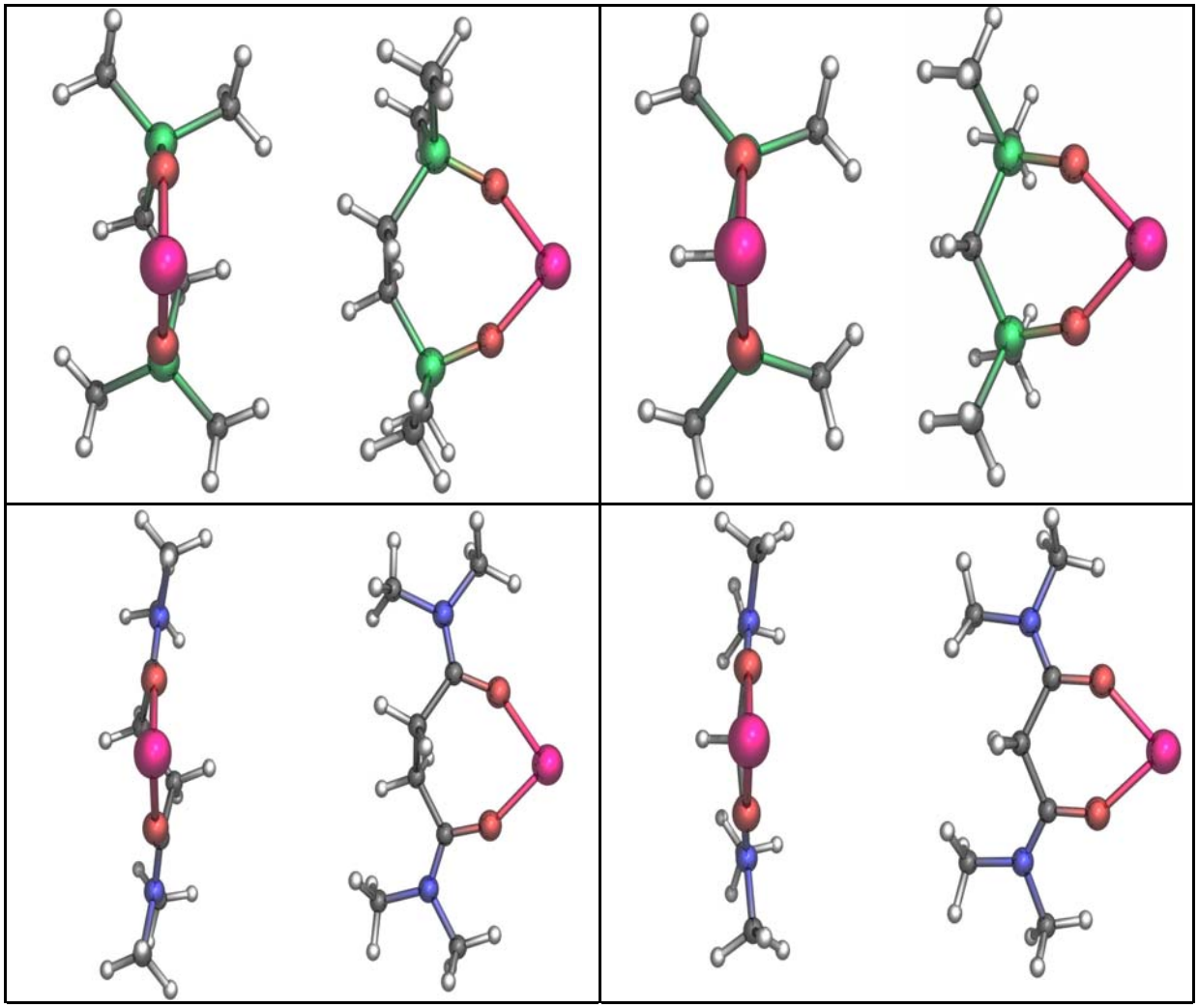

Figure S4. Optimized Eu·$\mathbf{L}^{3+}$ complexes (orthogonal views). From top left to bottom right: **L** = PccP, PcP, AccA and AcA.

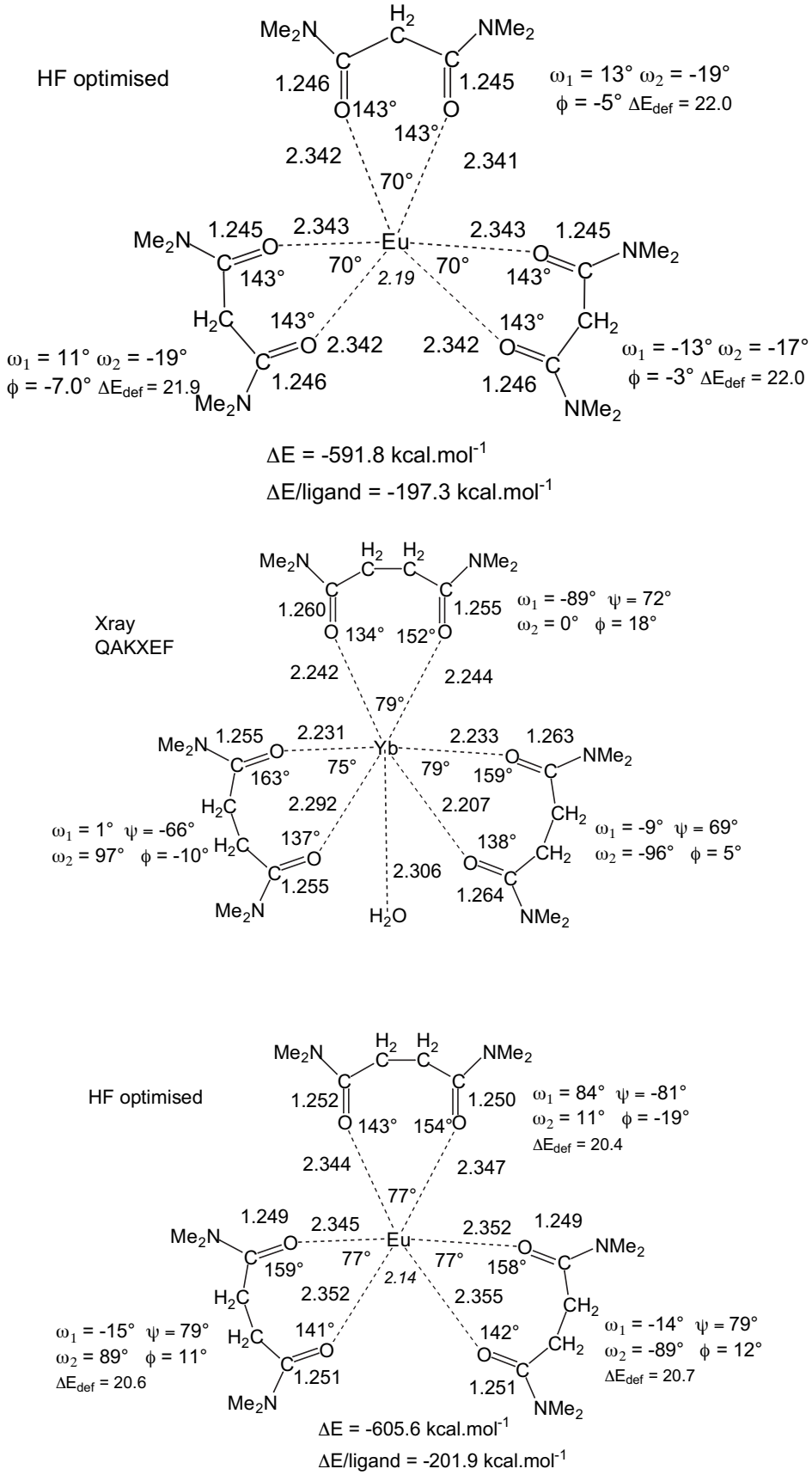

Figure S5. Optimized parameters of $Eu{\cdot}(AcA)_3^{3+}$ (top) and $Eu{\cdot}(AccA)_3^{3+}$ complexes and Xray structure of the QAKXEF **Yb(H$_2$O)(AccA)$_3$** complex. ΔE_{def} is the deformation energy of **L** (kcal/mol).

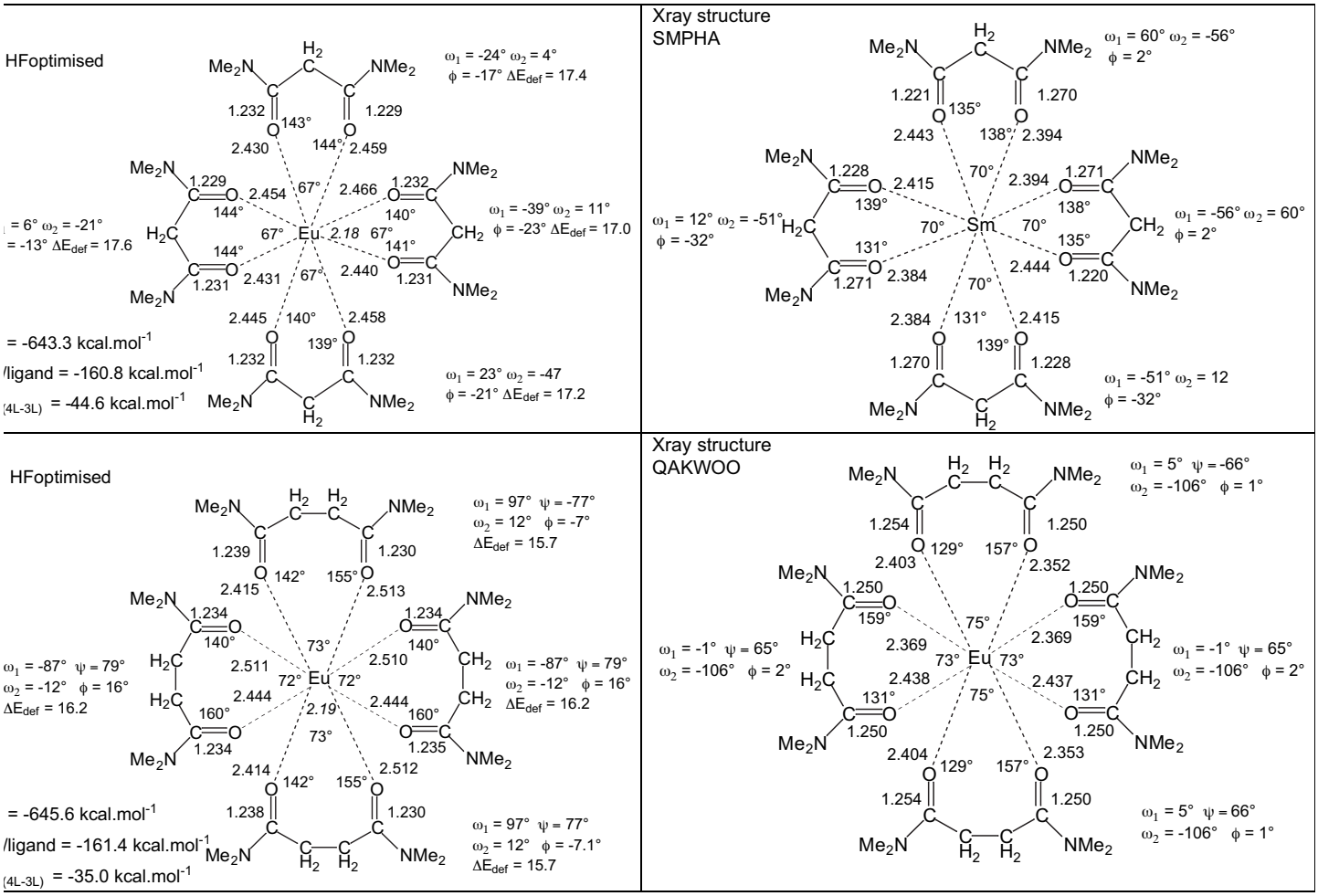

Figure S6. Optimized parameters of $Eu{\cdot}(AcA)_4^{3+}$ (top) and $Eu{\cdot}(AccA)_4^{3+}$ complexes and Xray structure of the SMPHA $Sm{\cdot}(AcA)_4^{3+}$ and QAKWOO $Eu{\cdot}(AccA)_4^{3+}$ complexes. ΔE_{def} is the deformation energy of **L** (kcal/mol).

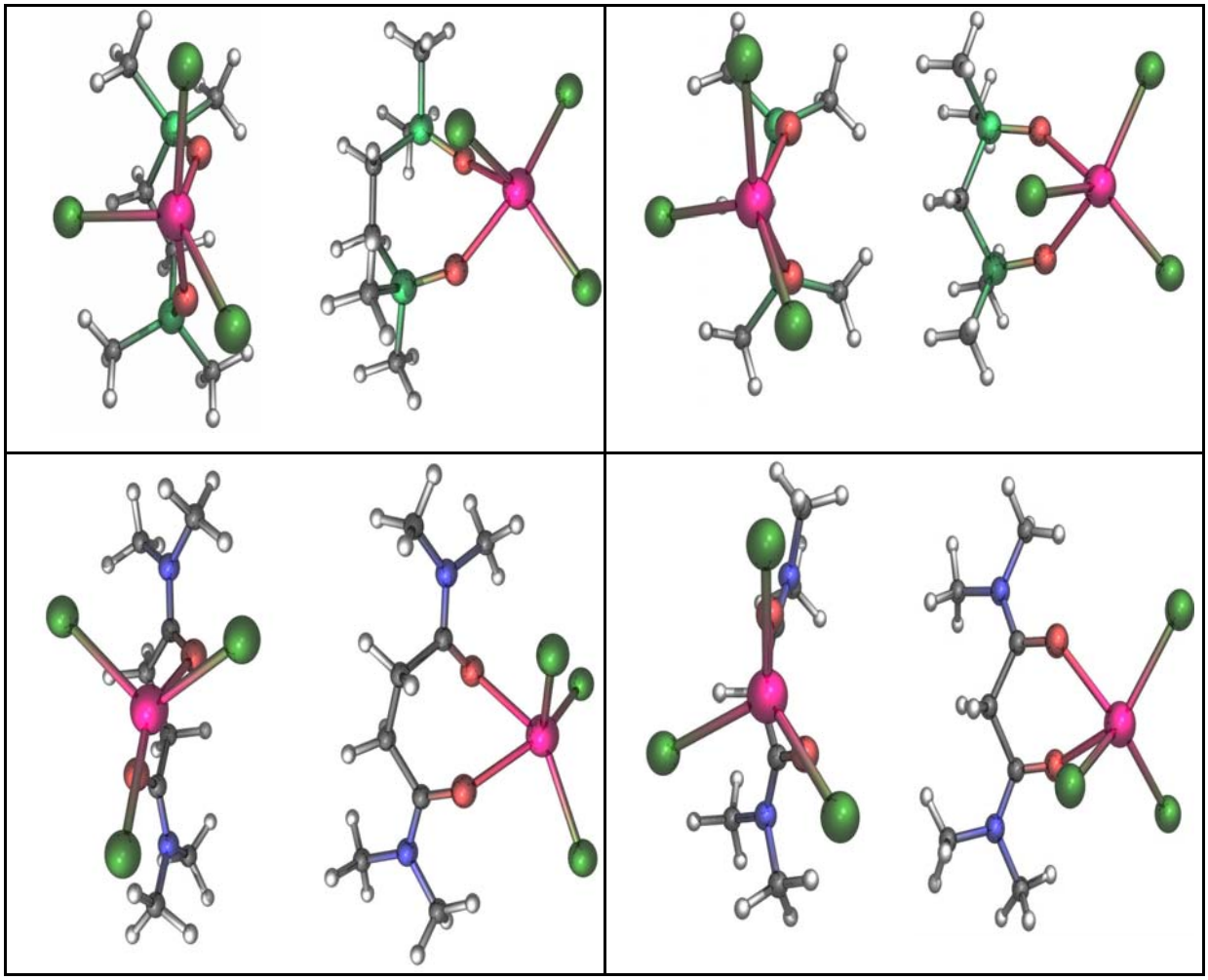

Figure S7. Optimized $EuCl_3 \cdot \mathbf{L}^{3+}$ bidentate complexes (orthogonal views). From top left to bottom right: **L** = PccP, PcP, AccA and AcA.

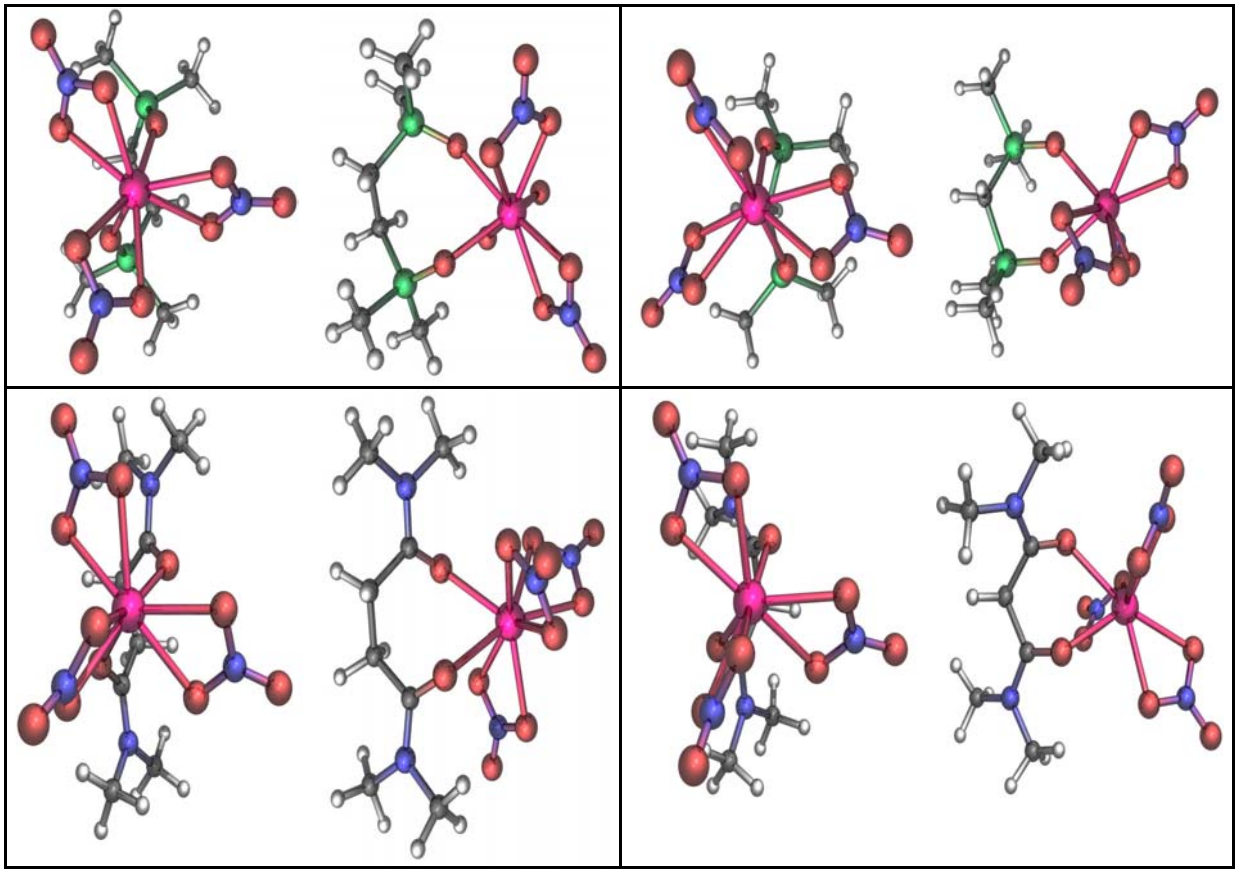

Figure S8. Optimized $Eu(NO_3)_3$·**L** bidentate complexes (orthogonal views). From top left to bottom right: **L** = PccP, PcP, AccA and AcA.

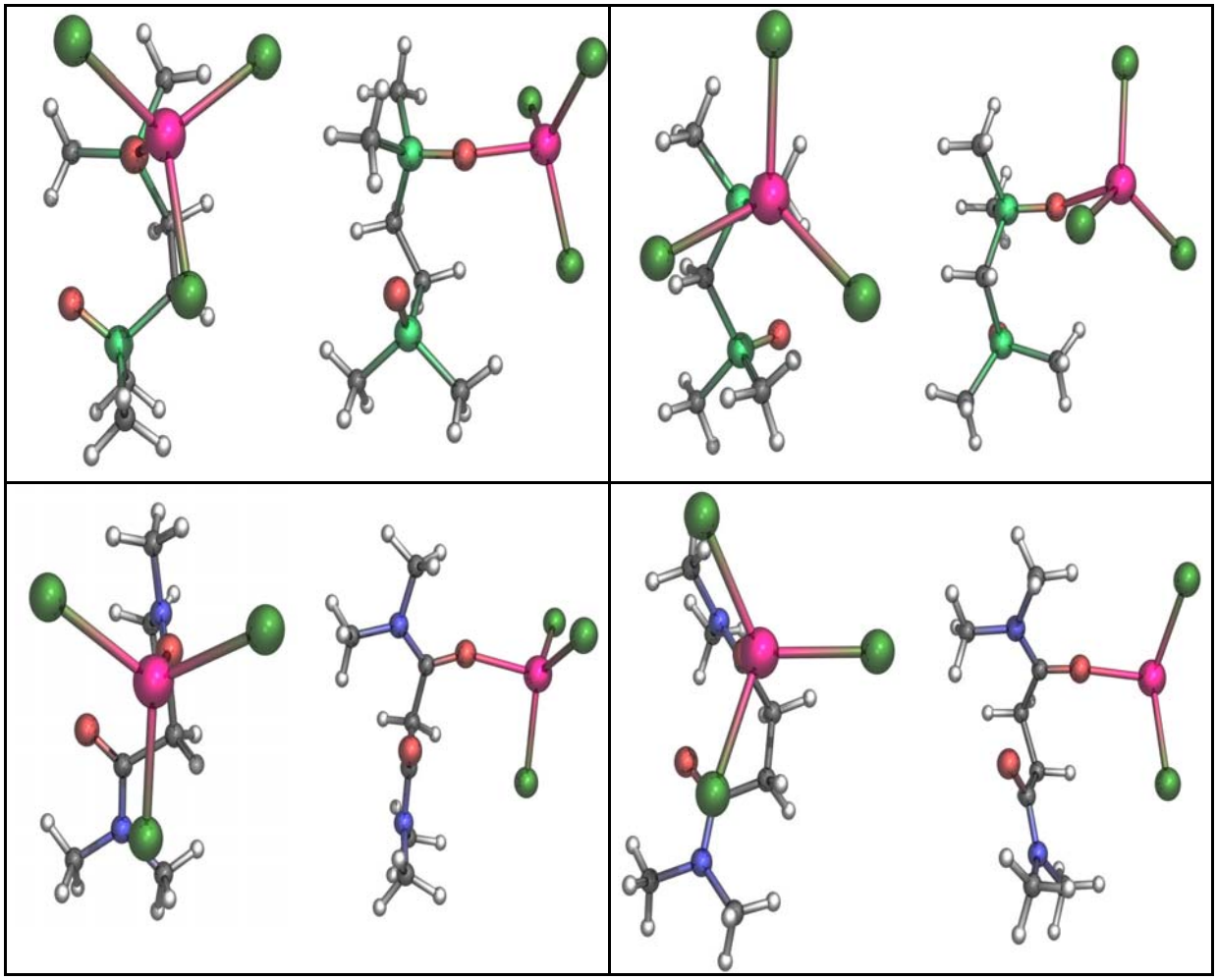

Figure S9. Optimized $EuCl_3 \cdot \mathbf{L}^{3+}$ monodentate complexes (orthogonal views). From top left to bottom right: **L** = PccP, PcP, AccA and AcA.

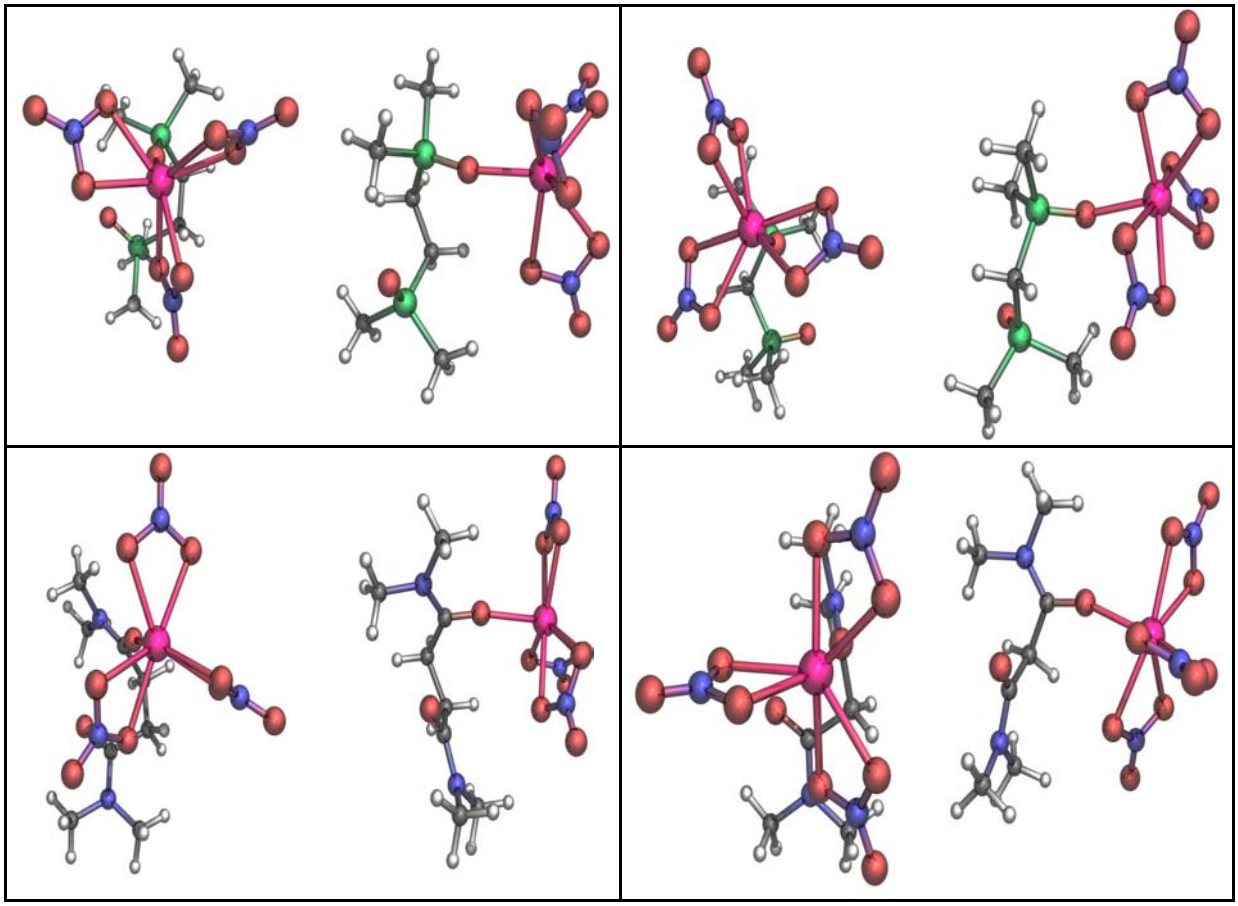

Figure S10. Optimized $Eu(NO_3)_3 \cdot \mathbf{L}$ monodentate complexes (orthogonal views). From top left to bottom right: **L** = PccP, PcP, AccA and AcA.